

Utilization of coal fly ash waste for effective recapture of phosphorus from waters

Rui Xu ^{1,2}, Tao Lyu ^{*3}, Lijing Wang ⁴, Yuting Yuan ⁵, Meiyi Zhang ⁶, Mick Cooper ⁷, Robert J.G. Mortimer ^{8,9}, Queping Yang ^{1,2}, Gang Pan ^{*6,7,9}

¹ *Chinese Research Academy of Environmental Sciences, Beijing 100012, China*

² *National Joint Research Center for Yangtze River Conservation, Beijing 100012, China*

³ *Cranfield Water Science Institute, Cranfield University, College Road, Cranfield, Bedfordshire MK43 0AL, United Kingdom*

⁴ *College of Resources and Environment, University of Chinese Academy of Sciences, Beijing 100049, China*

⁵ *UNSW Water Research Centre, School of Civil and Environmental Engineering, The University of New South Wales, Sydney, NSW 2052, Australia*

⁶ *Research Center for Eco-Environmental Sciences, Chinese Academy of Sciences, Beijing 100085, China*

⁷ *School of Animal, Rural and Environmental Sciences, Nottingham Trent University, Brackenhurst Campus, Nottinghamshire NG25 0QF, United Kingdom*

⁸ *School of Humanities, York St John University, Lord Mayor's Walk, York YO31 7EX, United Kingdom*

⁹ *Nanjing Xianglai Academy of Eco-environmental Science and Technology, Nanjing 210046, China*

*Corresponding authors: gang.pan@ntu.ac.uk (G.P.), t.lyu@cranfield.ac.uk (T.L.)

Abstract

Reutilisation of the waste by-products from industrial and agricultural activities is crucially important towards attainment of environmental sustainability and the 'circular economy'. In this study, we have developed and evaluated a sustainably-sourced adsorbent from coal fly ash, which was modified by a small amount of lanthanum (La-FA), for the recapture of phosphorous (P) from both synthetic and real natural waters. The prepared La-FA adsorbent possessed typical characteristic diffraction peaks similar to zeolite type Na-P1, and the BET surface area of La-FA was measured to be 10.9 times higher than that of the original FA. Investigation of P adsorption capability indicated that the maximum adsorption (10.8 mg P g^{-1}) was 6.14 times higher than that (1.8 mg P g^{-1}) of the original fly ash material. The ζ potentials measurement and P K-edge X-ray Absorption Near Edge Structure (XANES) spectra demonstrated that P was bonded on La-FA surfaces via an adsorption mechanism. After applying the proposed adsorbent to real lake water with La/P molar ratios in the range from 0.5:1 to 3:1, the La-FA adsorbent showed the highest phosphate removal ability with a La/P molar ratio 1:1, and the P adsorption was similar to that performance with the synthetic solution. Moreover, the La-FA adsorbent produced a negligible effect on the concentrations of total dissolved nitrogen (TDN), $\text{NH}_4^+\text{-N}$ and $\text{NO}_3^-\text{-N}$ in water. This study thus provides a potential material for effective P recapture and details of its operation.

Keywords: Circular economy; coal fly ash; eutrophication management, lanthanum modification; phosphorus adsorbent

1. Introduction

Along with the growth in global population and concurrent industrialization, the widespread application of phosphorus (P) as fertilizer and animal feed have resulted in substantially increased discharge of P into the environment and intensified episodes of eutrophication in natural waters (Conley et al., 2009; Pan et al., 2018; Smith et al., 1999). It has been reported that eutrophication could even occur at P concentrations as low as 0.02 mg P L^{-1} (Fernandez et al., 2007). Traditional and enhanced processes for the biological removal of P during natural and waste water treatments are generally not able to sustainably achieve such low effluent P concentrations (Kumar et al., 2019). The dosing of aluminium- or iron-based salts is a common approach in sewage treatment plants in order to secure an ultra-low level effluent with respect to P (Nakarmi et al., 2020; White et al., 2021). However, as P is a non-renewable resource, not only removal, but also recovery and recapture of the discharged P is strategically important for environmental sustainability (Pan et al., 2020). Therefore, treatment by adsorption is often suggested, due to the multiple advantages of low carbon footprint, minimal waste generation and the further option for P recovery (Kang et al., 2003).

Various synthetic adsorbents for P have been developed, and the valorisation of waste by-products from industrial and agricultural activities has recently drawn substantial attention within the concept of the circular economy (Zamparas et al., 2020). Many raw solid wastes (Table 1), such as steel slag (Bowden et al., 2009), magnesite dust (Al-Mallahi et al., 2020), concrete powder (Liu et al., 2020), and fine-grained by-products (Kasprzyk et al., 2021), have been investigated for P removal. In addition to the immediate advantage of low cost, some of these materials possess high porosity and mineral mixtures consisting of aluminium and other metal oxides, and have yielded P removal capabilities comparable to those of synthetic adsorbents. As coal combustion is still one of the most important sources of energy, the global generation of fly ash is estimated to be approximately 750 million tons, and thus the treatment/utilisation of these wastes is crucial (Blissett & Rowson, 2012). It is necessary to find a feasible way for the utilization of fly ash. Additionally, the complexity and variety of fly ash should

also be taken into consideration since it comprised of hundreds of different individual minerals and mineral groups (Vassilev and Vassileva, 2005).

Currently, researchers have attempted to use the raw fly ash for P removal. Some approaches have been used to improve the removal ability of modified fly ash through pre-treatment of acid/alkaline solutions and modification by metal ions (Hermassi et al., 2020). Although the modified fly ash could achieve P adsorption from several to hundreds of mg P g⁻¹ (Li et al., 2006; Wang et al., 2016b), it is considered that the overall efficiency could be improved further. The use of lanthanum (La), an environmentally friendly and relatively abundant rare earth element, is currently being used commercially to synthesise the P adsorbent *Phoslock*[®]. As a modifier on bentonite for P removal, a small portion of La (*ca.* 5.6%) could lead to P adsorption up to 10.6 mg P g⁻¹ due to its excellent P-binding ability (Haghseresht et al., 2009). A La-based P adsorbent could also overcome adverse effects of fluctuating pH and redox conditions in solution, attributable to strong P binding reactions (Wang et al., 2016b; Shin et al., 2005; Zhang et al., 2016), however, research into the use of La as modifier on fly ash for P removal is still not sufficient. It is therefore hypothesised that fly ash doped with a relatively small amount of La would result in a superior, low cost, and environmentally-friendly P adsorbent.

In many experiments demonstrating novel P adsorbents, adsorption capabilities are invariably tested using a synthetic P-contaminated solution with initial concentrations ranging from tens to hundreds mg P L⁻¹ (Xu et al., 2020). However, the P concentrations in natural waters or sewage effluent from upstream biological/chemical P removal treatments are usually much lower, for example in the range 0.1-1.0 mg P L⁻¹ (Wang et al., 2016a). Moreover, the removal efficiency of P from real waters could be affected by the presence of competing ions, such as SO₄²⁻ and CO₃²⁻ (Dithmer et al., 2016; Zhang et al., 2016). Previous studies, shown in Table 1, have reported a *ca.* 10% lower P removal ability from real wastewaters compared with that obtained from synthetic wastewater under the same condition. When targeting a real-life deployment, it should

be realised that little is known about the behaviour and mechanisms of P removal by the proposed La-modified fly ash adsorbent from both synthetic and natural real waters.

In order to address these knowledge gaps, the aims of this study were to develop a La-modified adsorbent from solid waste coal fly ash and to investigate its performance for P recapture from examples of both synthetic and real waters. Adsorption capacity, kinetics and isotherm characteristics, and the effect of pH on P adsorption, were initially investigated with synthetic water samples. The P K-edge X-ray Absorption Near Edge Structure (XANES) technique was employed to explore and characterise the microstructures formed when P bonded onto the proposed adsorbent. Moreover, the P removal performance of this material was also investigated with real lake waters, in order to provide an evidence, base that can be referenced regarding further implementations.

1 **Table 1.** Summary of the performance of various waste materials for P removal.

Material	Experiment solution	Dosage (g L ⁻¹)	pH	Initial P (mg P L ⁻¹)	P removal (%)	P adsorption capacity (mg P g ⁻¹)	Reference
Fly ash	Synthetic	2	3-11	30-300	100	-	(Shuai Gu et al., 2021)
	Real	2	-	51.5	100	-	
Steel slag	Synthetic	40	-	0-100	>90	1.14-2.49	(Barca et al., 2012)
	Real	40	-	0.41-1.11	>90	0.14-2.50	
	Synthetic	-	2-12	1-50, 100-300	62	8.39	(Bowden et al., 2009)
Eggshell	Synthetic	20	-	0.5-3.0	90	121	(Torit & Pihusut, 2019)
	Real	50	7.3	1.7	80	-	
	Synthetic	0.96	-	-	96.2	3.32	(Cy & Lpv, 2019)
Mussel shell	Synthetic	0-80	1.5-9.5	0-20	-	6.95	(Xiong et al., 2011)
Oyster shell	Synthetic	6	7.0-12	11.9	98	-	(Lee et al., 2009)
	Synthetic	400	-	6-80	-	32.9	(Wang et al., 2013)
Orange waste gel (loaded with zirconium)	Synthetic	1.67	1-9	-	-	57	(Biswas et al., 2008)
Magnesite dust	Synthetic	22.2	9	665	63%	-	(Al-Mallahi et al., 2020)
Concrete powder	Synthetic	-	10.5	20	-	4.96	(Liu et al., 2020)
Broken bricks	Synthetic	400	-	6-80	-	0.59	(Wang et al., 2013)
Iron humate	Synthetic	10-40	-	3.1-124	-	3.4-11.5	(Jano et al., 2011)
Fine-grained by-product	Synthetic	10	-	97.3	97.8	9.58	(Kasprzyk et al., 2021)

2

2. Materials and methods

2.1. Material preparation and characterisation

Raw coal fly ash (FA) was obtained from a power plant in Datong City (Shanxi province, China). The ash was washed three times with deionized water, dried at 105 °C, then passed through a 180 mesh sieve before use. La-modified fly ash (La-FA) was synthesized by the following process. The FA was first treated with 2.0 mol L⁻¹ NaOH solution at 95 °C for 24 h at a liquid/solid ratio of 360 mL alkali solution per 60 g FA, to obtain the zeolite and waste alkaline solution. After cooling to about 25 °C, a LaCl₃ solution (0.23 mol L⁻¹, 100 mL) was added dropwise to the mixture with continuous stirring, and the mixture further stirred for another 4 h at 25 °C. Finally, the resulting solid was washed three times with deionized water and freeze-dried over 24 h.

To obtain the exact content of La in the prepared La-FA, samples were digested in HF-HClO₄-HNO₃ solution and the chemistry of each resultant solution was determined by inductively coupled plasma optical emission spectrometry (ICP-OES, Optima 8300, PerkinElmer, USA). The morphologies of the raw FA and La-FA materials were observed by field emission scanning electron microscopy (FESEM, SU 8020, Hitachi, Japan). X-ray powder diffraction patterns were recorded on an X'Pert PRO MPD X-ray diffractometer (Malvern Panalytical, The Netherlands) with Cu-K radiation ($\lambda = 1.5408$) at 40 kV and 40 mA in the 2θ range of 5° to 90°. Brunauer-Emmett-Teller (BET) surface areas and pore size distributions were examined by a Micromeritics ASAP 2020 static volumetric analyser (Micromeritics Instrument Corp., Norcross, USA). Zeta (ζ) potential analysis of samples was performed by Zetasizer Nano ZS potential analyzer (Malvern Panalytical Ltd., United Kingdom).

2.2. P adsorption experiment

2.2.1. Adsorption isotherm

P adsorption isotherm experiments were conducted in 50 mL polypropylene tubes. Samples of FA and La-FA (1.0 g L⁻¹) were mixed with solutions containing various

concentrations of KH_2PO_4 each with 0.01 mol L^{-1} NaCl ionic background. The solution pH was adjusted to 8.50 ± 0.05 with 0.01 mol L^{-1} HCl and NaOH . The suspensions were shaken at $25 \text{ }^\circ\text{C}$ for 48 h. The suspensions were then centrifuged, filtered through $0.45 \text{ }\mu\text{m}$ membrane filters, and the clear supernatants used to determine P concentrations by the ascorbic acid method, using a UV-756 PC spectrophotometer at 880 nm (Shanghai Sunny Hengping Scientific Instrument Co. Ltd., China).

In order to model the adsorption results, Langmuir (Eq. 1) and Freundlich (Eq. 2) isotherms were used in this study, respectively.

$$q_e = \frac{q_m k_L c_e}{1 + k_L c_e} \quad (1)$$

$$q_e = K_F C_e^{1/n} \quad (2)$$

Where q_e is the equilibrium adsorption capacity (mg g^{-1}), q_m refers to the maximum adsorption capacity (mg g^{-1}), C_e is the equilibrium concentration after adsorption (mg L^{-1}), K_L is the constant in Langmuir model (L mg^{-1}), K_F is the constant in Freundlich model (mg g^{-1}), n is the constant in Freundlich isotherm model representing adsorption intensity.

2.2.2. Adsorption kinetics and desorption experiments

Adsorption kinetic experiments were carried out in 1000 mL flasks containing 500 mL P solution with concentrations of 10 and 30 mg P L^{-1} , and 0.5 g adsorbent samples added. The flasks were shaken at $25 \text{ }^\circ\text{C}$ for 48 h at 170 rpm. About 0.5 mL of each supernatant was sampled at various time intervals in order to determine P concentration. The pH was maintained at 8.50 ± 0.05 during the 48 h equilibration time.

Pseudo-second order kinetics (Eq. 3) and intra-particle diffusion (Eq. 4) models were used to model the experimental data, respectively.

$$\frac{t}{q_t} = \frac{1}{k_2 q_e^2} + \frac{t}{q_e} \quad (3)$$

$$q_t = k_i t^{1/2} \quad (4)$$

Where q_e and q_t represents the equilibrium capacity (mg g^{-1}) and adsorption amount versus

time t (min), k_2 is the equilibrium rate constant of pseudo-second-order adsorption ($\text{g mg}^{-1} \text{h}^{-1}$), k_i is the rate constant of intra-particle diffusion model ($\text{mg g}^{-1} \text{h}^{-1/2}$).

At the conclusion of the adsorption kinetics experiment, the exhausted solutions of La-FA samples with initial P concentration 30 mg P L^{-1} were first centrifuged, and 10 mL of the suspension at the bottom were preserved, then NaCl solution (0.01 mol L^{-1}) was added in order to maintain the same ionic strength. The suspensions were then shaken at $25 \text{ }^\circ\text{C}$ for 48 h. After that, the P concentrations of the clear supernatants were measured in order to determine the P desorption ability of the adsorbent.

2.3. The effect of pH on P removal

In order to assess the effect of pH on the equilibrium adsorption capacity, adsorption of P onto La-FA was conducted at pH 4, 5, 6, 7, 8, 9, and 10. La-FA (1.0 g L^{-1}) was added to 50 mL polypropylene tubes with an initial P concentration of 30 mg P L^{-1} with NaCl (0.01 mol L^{-1}) ionic background, and shaken at 170 rpm at $25 \text{ }^\circ\text{C}$ for 48 h. The solution pH was maintained with 0.01 mol L^{-1} HCl and NaOH.

2.4. P K-edge XANES data collection and analysis

The P K-edge XANES data were collected in fluorescence yield mode on Beamline 4B7A at the Beijing Synchrotron Radiation Facility (BSRF), China. Measurements were acquired at energies between -30 to $+90 \text{ eV}$ relative to P K-edge energy of 2152 eV with a minimum step size of 0.3 eV over the range 2140 and 2180 eV . XANES spectra of samples were normalized by the ATHENA software program (Ravel & Newville, 2005).

2.5. P binding experiments in real lake water

Real lake water was collected from Meiliang Bay of Taihu Lake (Jiangsu province, China) in November 2017. Taihu Lake is a mild eutrophic surface water and experiences periodic algal blooms every few years (Pan et al., 2019). In total, 5.0 L sample was collected by a plexiglass water sampler (Bei Jing Gresp Co., Ltd, China)

from 0.5 m deep below the surface in the centre of Meiliang Bay (31°43'N, 120°14'E). The water sample was first screened by a 180 µm mesh to remove large zooplankton grazers and then stored under 4 °C before being used for the following experiment. The chemical characteristics of the lake water are listed in Table 2. Stock suspensions of La-FA were prepared by continuous mixing of the adsorbent materials (50 mg) with deionized water (500 mL). Subsamples of 0.3, 0.6, 1.2, 1.8 and 2.4 mL were taken from these suspensions to obtain the desired adsorbent dosages, and then transferred to 50 mL polypropylene tubes containing lake water samples (40 mL) previously filtered through 0.45 µm membrane filters. The final volume of each solution was maintained at 45 mL by addition of aliquots of real lake water. The suspensions were shaken at 25 °C for 48 h at 170 rpm and then filtered for the measurement of total dissolved phosphorus (TDP), orthophosphate (PO₄³⁻-P), total dissolved nitrogen (TDN), ammonia nitrogen (NH₄⁺-N) and nitrate nitrogen (NO₃⁻-N). Each experiment was carried out in triplicate.

Table 2 Characteristics of the natural water used in the P adsorption experiment.

Parameter	Average value
pH	7.85
Dissolved oxygen (DO, mg O ₂ L ⁻¹)	8.50
Electrical conductivity (µS cm ⁻¹)	180
Total phosphorus (TP, mg P L ⁻¹)	0.067
Total dissolved phosphorus (TDP, mg P L ⁻¹)	0.030
Orthophosphate (PO ₄ ³⁻ -P, mg P L ⁻¹)	0.011
Total nitrogen (TN, mg N L ⁻¹)	2.09
Total dissolved nitrogen (TDN, mg N L ⁻¹)	2.02
Nitrate nitrogen (NO ₃ ⁻ -N, mg N L ⁻¹)	1.54
Ammonia nitrogen (NH ₄ ⁺ -N, mg N L ⁻¹)	0.13
Dissolved organic carbon (DOC, mg L ⁻¹)	10.25

3. Results and discussion

3.1. Characterisation of the La-modified coal fly ash

The original FA particles were characterised by spherical morphologies and smooth surfaces, whereas particles of La-FA exhibited more irregular structures and much rougher surfaces (Fig. 1A). FESEM images indicated that particle size distributions of

La-FA adsorbents were not uniform, with most average particle sizes of approximately 20 μm . The proportion of La in La-FA was approximately 5.0% (w/w), which was slightly lower than that contained in the commercial La based P adsorbent, *Phoslock*[®] (5.6%; Xu et al., 2017). These differences could be ascribed mainly to the formation of zeolite crystal clusters during the La modification process. XRD analysis (Fig. 1B) suggested that the original FA possessed crystalline phases of mullite ($3\text{Al}_2\text{O}_3 \cdot 2\text{SiO}_2$ or $2\text{Al}_2\text{O}_3 \cdot \text{SiO}_2$), quartz (SiO_4), hematite (Fe_2O_3) and corundum (Al_2O_3), which were also observed in the structures of La-FA. In addition, La-FA particles showed typical characteristic diffraction peaks similar to zeolite type Na-P1 ($\text{Na}_6\text{Al}_6\text{Si}_{10}\text{O}_{32} \cdot 12\text{H}_2\text{O}$, JCPDS code 39-0219) at $2\theta = 12.455^\circ$, 17.649° , 21.657° , 28.072° , and 33.356° . However, the characteristic diffraction peaks of La-(hydro)oxide were not detected in La-FA, possibly owing to its existence in an amorphous phase (Wang et al., 2016b).

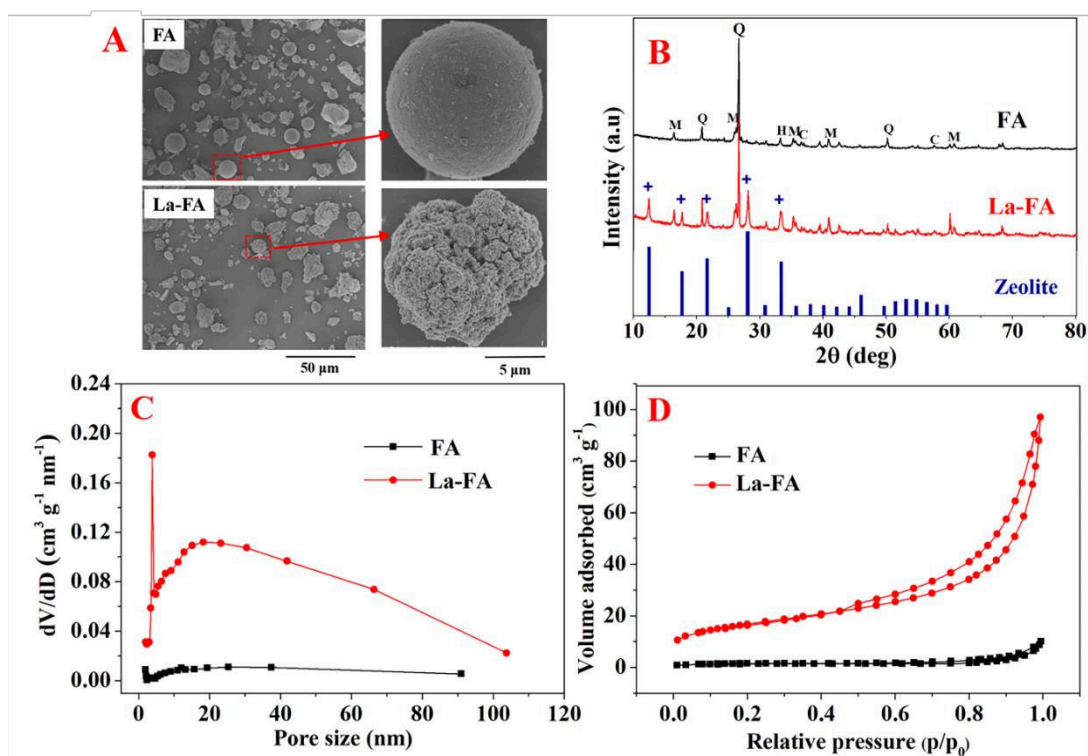
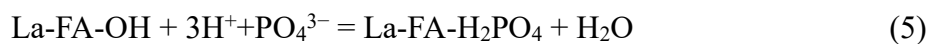


Fig. 1. (A) SEM images of original FA and La-FA. (B) XRD patterns of original FA, La-FA, and zeolite identifying selected peaks of minerals quantified by Rietveld analysis (M = mullite, Q = quartz, H = hematite, C = corundum). (C) Pore size distribution of original FA and La-FA. (D) N_2 adsorption/desorption isotherm of original FA and La-FA.

It has been reported that zeolite and hydrous La-oxide possesses a narrow pore size distribution around 4.0 nm (Wang et al., 2016b). This data supports findings from this study of a pore size distribution around 3.9 nm in La-FA (Fig. 1C), which was mainly dependant on the pore structure of La-(hydro)oxide. The N₂ adsorption-desorption isotherm of La-FA could be represented by a typical curve of type II (Fig. 1D). The BET surface area of La-FA was measured at 59.9 m² g⁻¹, which was 10.9 times larger than that of the original FA (5.5 m² g⁻¹), and in turn, was higher than that determined for a lanthanum-doped coal fly ash-blast furnace cement composite with a surface area of 11.4 m² g⁻¹ (Asaoka et al., 2020). Additionally, the pore volume of La-FA was calculated to be 0.11 cm³ g⁻¹, which was 11.0-fold larger than that of the original FA material, with a pore volume of 0.01 cm³ g⁻¹. Compared with the original FA, the obvious increases in BET surface area and pore volume of La-FA have further demonstrated the potential enhanced capabilities for P adsorption of the latter material.

3.2 P adsorption behaviours and mechanism

At an initial P concentration of 30 mg P L⁻¹, La-FA exhibited the highest P adsorption capacity of 22.8 mg P L⁻¹ at pH 4.25, which gradually decreased to 9.6 mg P L⁻¹ along with increasing pH to 9.76 (Fig. 2A). The negative correlation between the P adsorption capacity and pH was supported by previous relevant studies (Awual et al., 2011a; Goscianska et al., 2017), and which may have been due to the increased hydroxide concentration that might potentiate interference with the hard Lewis acid anion in water, thus affecting P adsorption (Awual et al., 2011c). Moreover, hydrogen ions might transfer to the surface of La-FA for capturing the dominant species of H₂PO₄⁻ and HPO₄²⁻ according to the following reactions (Eq. 5) and (Eq. 6) (Awual et al., 2011b; Hiemstra and Van Rimsdijk, 1996).



In order to simulate the scenario of P removal from eutrophic natural waters, a pH of 8.50 was chosen in the following experiments (Xiong & Peng, 2008). The capacities

for P adsorption, by the original FA and La-FA materials, increased with contact time at initial P concentrations of 10 and 30 mg P L⁻¹ and attained equilibrium after about 30 h (Fig. 2B). The pseudo-second order kinetics model better fitted the results (r^2 of 0.992-0.997) compared with those (r^2 of 0.886-0.936) obtained from the intra-particle diffusion model (Table 3). The rate constants (k_2) of the original FA and La-FA were calculated at 2.756 and 0.058 g mg⁻¹ h⁻¹, under an initial P concentration of 10 mg L⁻¹, respectively. The rate constant for La-FA further decreased to 0.035 g mg⁻¹ h⁻¹ when the initial P concentration increased to 30 mg P L⁻¹.

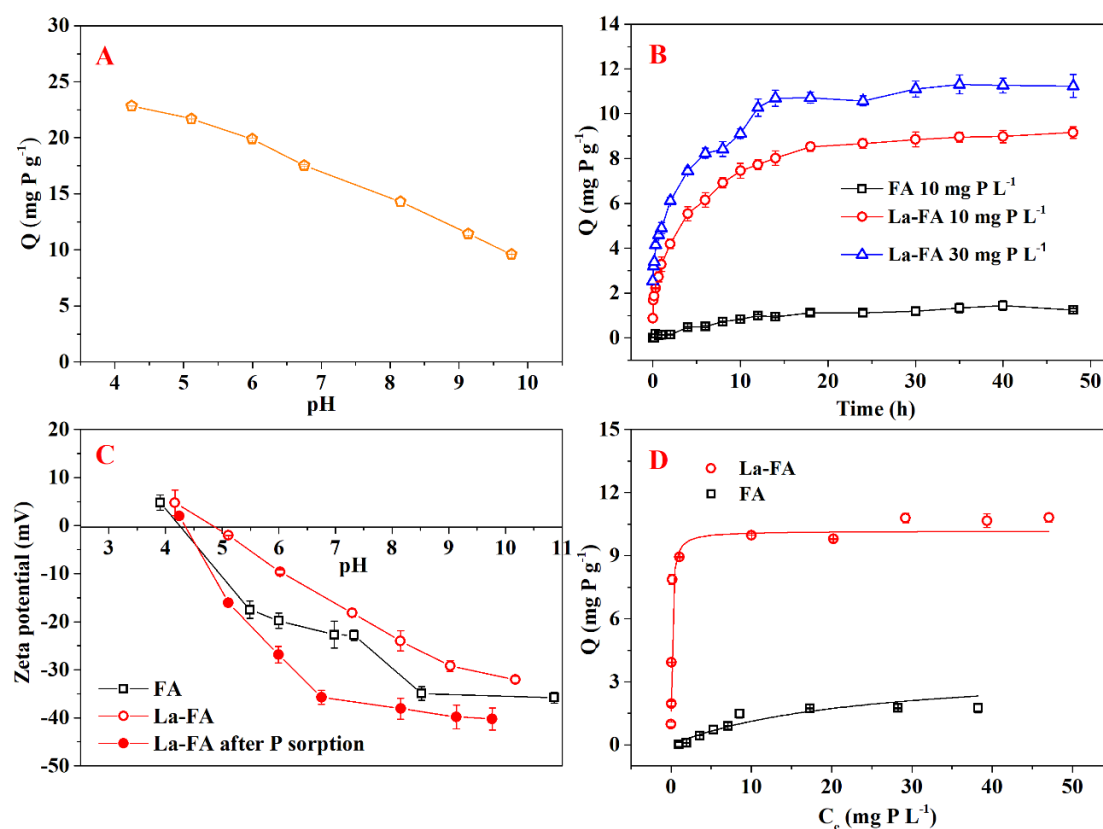


Fig. 2. (A) Effect of pH on P adsorption efficiency for La-FA. (B) Kinetic studies for P adsorption by original FA and La-FA. (C) The ζ potentials of original FA, La-FA and La-FA after P adsorption. (D) Langmuir adsorption isotherms of P by original FA and La-FA.

Table 3. Pseudo-second order and intra-particle diffusion model parameters of P adsorption by original FA and La-FA.

Adsorbent	Initial P concentration (mg P L ⁻¹)	Pseudo-second order model			Intra-particle diffusion model	
		k_2 (g mg ⁻¹ h ⁻¹)	q_e (mg P g ⁻¹)	r^2	k_i (mg g ⁻¹ h ^{-1/2})	r^2
FA	10	2.756	0.378	0.992	0.236	0.936
La-FA	10	0.058	9.390	0.997	1.256	0.891
La-FA	30	0.035	13.141	0.992	1.354	0.886

The ζ potentials of original FA and La-FA materials exhibited decreasing trends with increasing pH value (Fig. 2C). The ζ potentials of La-FA were higher than those of the original FA under similar conditions of pH, possibly owing to the presence of La-modified compounds (Goscianska et al., 2017). Additionally, the ζ potentials of La-FA after P adsorption all decreased compared to the initial values. For example, the initial ζ potential of La-FA was -24.0 mV at pH 8.15 and decreased to -38.1 mV after P adsorption. These results suggested that P might be bonded onto the surface of La-FA by formation of inner sphere complexes (Antelo et al., 2005; Wan et al., 2016).

When evaluating the P adsorption capacity by La-FA compared to the original FA, a Langmuir isotherm model presented clearly better fittings (r^2 of 0.994-0.999) compared with those (r^2 of 0.713-0.831) fitted by the Freundlich model (Table 4). The better Langmuir isotherm simulation is visualised in Fig. 2D, and the maximum adsorption capacity of La-FA was determined to be 10.8 mg P g⁻¹, some 6.1 times higher than that of the original FA (1.8 mg P g⁻¹). In accordance with previous studies, the molar ratio of adsorbed P to La was used to calculate the efficiency of La usage in La-modified materials (Emmanuelawati et al., 2013; Yang et al., 2012; Yang et al., 2011). In the present study, the molar ratio of adsorbed P to La in La-FA was 0.96, by the ratio of the maximum amount of P adsorbed, calculated by the Langmuir model (10.8 mg P g⁻¹), to the total La content in La-FA (5.0%). The molar ratio of P to La (1:1) in the La-FA material was also in agreement with previous studies (Yasseri & Epe, 2015).

Table 4. Langmuir and Freundlich isotherms parameters of P adsorption by original FA and La-FA.

Adsorbent	Langmuir			Freundlich		
	q_m (mg P g ⁻¹)	k_L (L mg ⁻¹)	r^2	n	k_F (mg P g ⁻¹)	r^2
FA	1.752	1.675	0.994	0.895	0.002	0.831
La-FA	10.753	2.981	0.999	4.417	50.188	0.713

In order to investigate and demonstrate the mechanism at the molecular level, the P K-edge XANES spectra of the La-FA sample containing bonded P was measured (Fig. 3A). As P has only one valance state, it can be perfectly characterised by the derivative analysis of the XANES spectra (Khare et al., 2007). It has been reported that aqueous Fe(III)-PO₄³⁻ solutions increased in the degree of bidentate compared to monodentate bonding with increasing Fe/P ratio by using ferrihydrite adsorbent (Filatova et al., 1976). However, in this study, there was no obvious change of white line energy from the La-FA bonded P sample, compared to the derivative spectra for HPO₄²⁻ (Fig. 3B), possibly indicating that P was bound on La-FA surfaces by adsorption (Khare et al., 2007). Although XANES is recognized as an element-specific and in-situ method for the detection of the molecular structures of reacting species (Khare et al., 2005; Xu et al., 2017), it is beneficial to explore molecular mechanisms by combining the results from multiple-characterisation methods, such as X-ray photoelectron spectroscopy (XPS), and Fourier transform infrared spectroscopy (FTIR), which could be conducted in a future study.

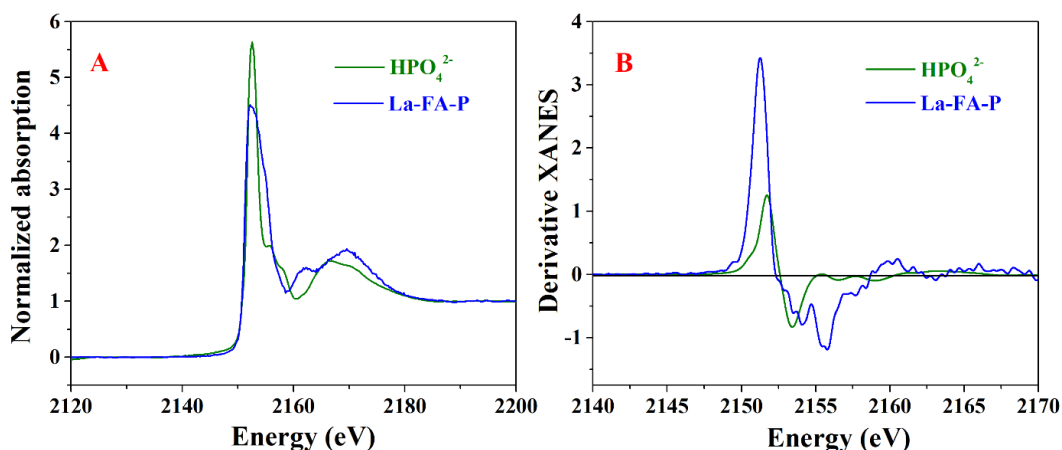


Fig. 3. (A) Normalized XANES spectra of HPO₄²⁻ and La-FA bonded with P. (B) First-derivative XANES spectra for HPO₄²⁻ and La-FA bonded with phosphate.

3.3. La-FA application in real natural waters

Previous studies have investigated the vertical distribution of La in-lake sediments for each experimental site, in order to explore the impact of *Phoslock*[®] being applied for remediation of eutrophic water bodies (Yasseri & Epe, 2015). Although the theoretical binding ratio of a La/P material was 1:1 based on the reaction equation ($\text{La}^{3+} + \text{PO}_4^{3-} = \text{LaPO}_4$), the application of materials with La/P molar ratios greater than 1:1 could increase P removal by up to 60% (Yasseri & Epe, 2015). Hence, it is suggested that more studies should be carried out in order to investigate the amount of La-modified material required in a real environmental application. Fig. 4 illustrates that the La-FA had a relatively efficient removal ability to PO₄³⁻-P at different La/P molar ratios compared with TDP. With La/P molar ratios of 0.5:1, 1:1, 1.5:1 and 2:1, PO₄³⁻-P removal efficiencies were $54.5 \pm 2.4\%$, $72.8 \pm 2.7\%$, $62.2 \pm 2.9\%$ and $63.6 \pm 1.8\%$, respectively. The La-FA material exhibited noticeably higher PO₄³⁻-P removal ability with a La/P molar ratio of 1:1 compared with that a La/P molar ratio of 0.5:1, which might suggest that this La/P molar ratio equalled the best theoretical value. Increasing the La/P to 1.5:1 and further to 2:1 did not produce significant differences in the PO₄³⁻-P removal abilities, which might have been caused by saturation of adsorption sites in the material. It should be noted that the current experiment was conducted in aqueous solution without the presence of sediment. Taking into consideration P liberated from

sediments, higher dosage of La-modified materials might be applied in lake restoration geo-engineering (Huang & Zhang, 2010). Nevertheless, the removal efficiency of TDP by La-FA increased with increasing La/P molar ratio. In detail, the removal rate of TDP was determined to be only $10.0 \pm 2.4\%$ with La/P molar ratio 0.5:1, but $63.2 \pm 1.8\%$ when the La/P molar ratio increased to 3:1 (Fig. 4A). In this study, La-FA exhibited better selectivity to $\text{PO}_4^{3-}\text{-P}$ than to TDP, possibly owing to presence of many other P species (e. g. hexakisphosphate) in the latter (Wan et al., 2016).

Previous studies have demonstrated that some La-modified materials (e. g. La-modified bentonite) could lead to adverse effects on the concentrations of nitrogen-containing compounds in water (Reitzel et al., 2013). The nutrients, including $\text{NH}_4^+\text{-N}$, $\text{NO}_3^-\text{-N}$, and $\text{NO}_2^-\text{-N}$ could attributed to the soluble fraction in the bentonite-based material and to the nitrification process, as occurs in anaerobic sediments (Van Oosterhout and Lürling, 2013; Gibbs et al., 2011). Such consequences might pose a risk to the surface waters, as N is also one of the key causes of eutrophication (Wang et al., 2016a; Zhang et al., 2018). In order to investigate the effect of La-FA material to nitrogen in natural water system, we also determined the concentrations of $\text{NH}_4^+\text{-N}$, $\text{NO}_3^-\text{-N}$ and TDN in water under different La-FA dosage regimes, which indicated that La-FA had little effect on the nitrogen concentrations in water (Fig. 4B). With increase in La/P molar ratio, TDN content of the solution did not change significantly, compared with the initial concentration of 2.02 mg N L^{-1} prior to adsorption (Table 2). Concentrations of $\text{NH}_4^+\text{-N}$ and $\text{NO}_3^-\text{-N}$ in the lake water was not noticeably affected by the addition of La-FA.

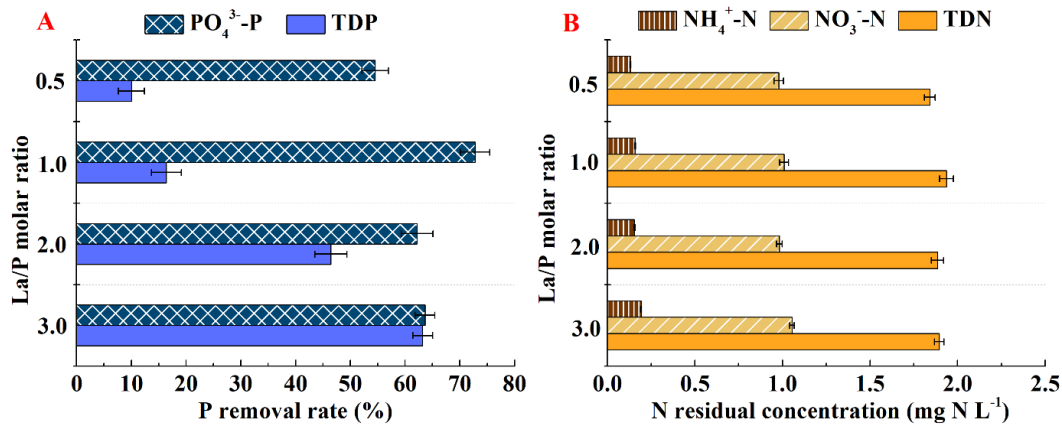


Fig. 4. (a) Removal rates of PO₄³⁻-P and TDP by La-FA. (b) Residual concentrations of NH₄⁺-N, NO₃⁻-N and TDN after using La-FA.

3.4 Environmental implications

Laboratory experiments on La-FA have provided the theoretical basis and a technical reference for its further application in a natural aquatic environment. The key purpose of lake geological engineering is to control a eutrophication problem quickly and effectively (Reitzel et al., 2013). The maximum amount of P adsorbed by La-FA (10.8 mg P g⁻¹, Fig. 4) was similar to that obtained by use of the commercially available material *Phoslock*[®] (10.6 mg P g⁻¹) (Haghseresht et al., 2009). However, as a material for the recapture of P for eutrophication control, the stability of the La-FA adsorbent should be considered when applied into natural waters. Here, La-FA showed great ability to combine with P, exhibiting a desorption rate of 0.81% without taking into consideration possible interference by submerged macrophytes in shallow waters (Zhang et al., 2018). To the best of our knowledge, there exist many ionic species in natural waters such as chloride, sulfate, calcium, magnesium, arsenic and nitrite (Shahat et al., 2018; Awual, et al., 2019), which might act as potential antagonists for efficient P adsorption. It has been reported that some hydrophobic materials, such as anion exchange fibres prefer lowly hydrated anions (H₂PO₄⁻) compared with highly hydrated ones (H₂AsO₄⁻) with the same electronic charge (Awual et al., 2008). In this study, as an effective P adsorption material, La-FA showed better selectivity and sensitivity to different P species for both synthetic and natural water systems (Fig. 4). However, the

effects of multiple different ions on efficiency of P removal by La-modified materials should be further considered when applying these to natural waters. Based on the current results of this study, longer-term experiments in large-scale systems should be further conducted in order to better investigate the selectivity to different ions and to evaluate the full cost-benefit of feasibility of waste utilization.

This study suggested that the proposed La-based material could provide a suitable approach for the reuse of this type of industrial wastes. In addition to removal of P, La-FA could provide a sediment covering function, possibly improving the anaerobic environment of sediment and effectively slowing down the release of nutrients in sediment. Practically, it would be necessary to determine the optimum dosage and proportion of La-modified materials used for a project, according to the different sediment environments present. As a natural lake system is very complex, investigation into the specific effects of different dosages of La-modified materials on natural aquatic organisms such as *Daphnia magna* and fish should be carried out. According to the different water quality conditions and the types of aquatic organisms, the ecological security of the aquatic organisms should be evaluated.

4. Conclusions

In this study, we have developed a La-modified adsorbent using solid waste coal fly ash (La-FA) as raw material and investigated its performance for removal of phosphorus from both synthetic and natural waters. The adsorption equilibrium data followed well the Langmuir model with maximum adsorption capacity 10.8 mg P g^{-1} of La-FA, some 6 times higher than that obtained from the original FA material. The pseudo-second-order kinetic model was identified as the best model to describe the adsorption process. Both the measurement of ζ potentials and P K-edge XANES spectra indicated that P was probably bonded onto the La-FA by surface adsorption. The La-FA showed the highest PO_4^{3-} -P removal ability at a La/P molar ratio of 1:1. The application of La-FA had negligible effects on the concentrations of TDN, NH_4^+ -N and NO_3^- -N in water. With these results, La-FA may be a potential material for the removal of P from polluted

natural waters for the mitigation of eutrophication.

Declaration of competing interest

The authors declare no conflicts of interest in this research.

Acknowledgements

This work was supported by National Key R&D Program of China (2017YFA0207204, 2018YFD0800305), National Natural Science Foundation of China (21377003), the Major Science and Technology Program for Water Pollution Control and Treatment (2018ZX07110004) and Joint Research Project for the Yangtze River Conservation (Phase I, 2019-LHYJ-01).

Reference

- Al-Mallahi, J., Sürmeli, R., Alli, B. 2020. Recovery of phosphorus from liquid digestate using waste magnesite dust. *J. Clean. Prod.*, **272**, 122616.
- Asaoka, S., Kawakami, K., Saito, H., Ichinari, T., Oikawa, T. 2020. Adsorption of phosphate onto lanthanum-doped coal fly ash-Blast furnace cement composite. *J. Hazard. Mater.*, **406**(2), 124780.
- Awual, M. R., Asiri, A. M., Rahman, M. M., Alharthi, N. H. 2019. Assessment of enhanced nitrite removal and monitoring using ligand modified stable conjugate materials. *Chem. Eng. J.*, 363, 64-72.
- Awual, M.R., El-Safty, S.A., Jyo, A. 2011a. Removal of trace arsenic (V) and phosphate from water by a highly selective ligand exchange adsorbent. *J. Environ. Sci.*, **23**, 1947-1954.
- Awual, M.R., Jyo, A. 2011b. Assessing of phosphorus removal by polymeric anion exchangers. *Desalination*, **281**(1), 111-117.
- Awual, M.R., Jyo, A., Ihara, T., Seko, N., Tamada, M., Him, K.T. 2011c. Enhanced trace phosphate removal from water by zirconium (IV) loaded fibrous adsorbent. *Water Res.*, **45**(15), 4592-4600.
- Awual, M. R., Urata, S., Jyo, A., Tamada, M., & Katakai, A. 2008. Arsenate removal

- from water by a weak-base anion exchange fibrous adsorbent. *Water Res.*, **42**(3), 689-696.
- Barca, C., Gérente, C., Meyer, D., Chazarenc, F., Andres, Y. 2012. Phosphate removal from synthetic and real wastewater using steel slags produced in Europe. *Water Res.*, **46**(7), 2376-2384.
- Biswas, B.K., Inoue, K., Ghimire, K.N., Harada, H., Ohto, K., H., K. 2008. Removal and recovery of phosphorus from water by means of adsorption onto orange waste gel loaded with zirconium. *Bioresource Technol.*, **99**, 8685-8690.
- Blissett, R.S., Rowson, N.A. 2012. A review of the multi-component utilisation of coal fly ash. *Fuel*, **97**, 1-23.
- Bowden, L.I., Jarvis, A.P., Younger, P.L., Johnson, K.L. 2009. Phosphorus removal from waste waters using basic oxygen steel slag. *Environ. Sci. Technol.*, **43**(7), 2476-2481.
- Conley, D.J., Paerl, H.W., Howarth, R.W., Boesch, D.F., Seitzinger, S.P., Havens, K.E., Lancelot, C., Likens, G.E. 2009. Controlling eutrophication: nitrogen and phosphorus. *Science*, **323**, 1014-1015.
- Cy, A., Lpv, B. 2019. Wasted salted duck eggshells as an alternative adsorbent for phosphorus removal. *J. Environ. Chem. Eng.*, **7**(6), 103443.
- Dithmer, L., Nielsen, U.G., Lundberg, D., Reitzel, K. 2016. Influence of dissolved organic carbon on the efficiency of P sequestration by a lanthanum modified clay. *Water Res.*, **97**(Jun.15), 39-46.
- Emmanuelawati, I., Yang, J., Zhang, J., Zhang, H.W., Zhou, L., Yu, C.Z. 2013. Low-cost and large-scale synthesis of functional porous materials for phosphate removal with high performance. *Nanoscale*, **5**(13), 6173-6180.
- Fernandez, F.J., Villase, J., Rodriguez, L. 2007. Effect of the internal recycles on the phosphorus removal efficiency of a WWTP. *Eng. Chem. Res.*, **46**, 7300-7307.
- Filatova, L.N., Shelyakina, M.A., Plachinda, A.S., Makarov, E.F. 1976. Dimerisation of iron (III) in aqueous solution in the presence of phosphate ions. *Russ. J. Inorg. Chem.* **21**, 1494-1497.

- Gibbs, M., M., Hickey, C., W., Özkundakci, D. 2011. Sustainability assessment and comparison of efficacy of four P-inactivation agents for managing internal phosphorus loads in lakes: sediment incubations. *Hydrobiologia*, **658**, 253-275.
- Goscianska, J., Ptaszkowska-Koniarz, M., Frankowski, M., Franus, M., Panek, R., Franus, W. 2017. Removal of phosphate from water by lanthanum-modified zeolites obtained from fly ash. *J. Colloid Interf. Sci.*, **513**, 72-81.
- Haghseresht, F., Wang, S., Do, D.D. 2009. A novel lanthanum-modified bentonite, Phoslock, for phosphate removal from wastewaters *Appl. Clay Sci.*, **46**(4), 369-375.
- Hermassi, M., Valderrama, C., Font, O., Moreno, N., Cortina, J.L. 2020. Phosphate recovery from aqueous solution by K-zeolite synthesized from fly ash for subsequent valorisation as slow release fertilizer. *Sci. Total Environ.*, **731**, 139002.
- Hiemstra, T., Van Rimsdijk, W.H. 1996. A surface structural approach to ion adsorption: The charge distribution (CD) model. *J. Colloid Interface Sci.*, **179**, 488-508.
- Huang, X.L., Zhang, J.Z. 2010. Spatial variation in sediment-water exchange of phosphorus in Florida Bay: AMP as a model organic compound. *Environ. Sci. Technol.*, **44**, 7790-7795.
- Jano, P., Kopecká, A., Hejda, S. 2011. Utilization of waste humate product (iron humate) for the phosphorus removal from waters. *Desalination*, **265**(1-3), 88-92.
- Kang, S.K., Choo, K.H., Lim, K.H. 2003. Use of iron oxide particles as adsorbents to enhance phosphorus removal from secondary wastewater effluent. *Sep. Sci. Technol.*, **38**, 3853-3874.
- Kasprzyk, M., Czerwionka, K., Gajewska, M. 2021. Waste materials assessment for phosphorus adsorption toward sustainable application in circular economy. *Resour. Conserv. Recy.*, **168**, 105335.
- Khare, N., Hesterberg, D., Martin, J. D. 2005. XANES investigation of phosphate sorption in single and binary systems of iron and aluminum oxide minerals. *Environ. Sci. Technol.* **39** (7), 2152-2160.

- Khare, N., Martin, J.D., Hesterberg, D. 2007. Phosphate bonding configuration on ferrihydrite based on molecular orbital calculations and XANES fingerprinting. *Geochim. Cosmochim. Ac.*, **71**(18), 4405-4415.
- Kumar, P.S., Korving, L., Loosdrecht, M., Witkamp, G.J. 2019. Adsorption as a technology to achieve ultra-low concentrations of phosphate: Research gaps and economic analysis. *Water Research X*, **4**, 100029.
- Lee, C.W., Kwon, H.B., Jeon, H.P., Koopman, B. 2009. A new recycling material for removing phosphorus from water. *J. Clean. Prod.*, **17**, 683-687.
- Li, Y.Z., Liu, C.J., Luan, Z.K., Peng, X.J., Zhu, C.L., Chen, Z.Y., Zhang, Z.G., Fan, J.H., Jia, Z.P. 2006. Phosphate removal from aqueous solutions using raw and activated red mud and fly ash. *J. Hazard. Mater.*, **137**(1), 374-383.
- Liu, D., Zhu, H., Wu, K., Wang, F., Liao, Q. 2020. Understanding the effect of particle size of waste concrete powder on phosphorus removal efficiency. *Constr. Build. Mater.*, **236**, 117526.
- Nakarmi, A., Viswanathan, T., Bourdo, S.E., Watanabe, F., Moreira, R. 2020. Removal and recovery of phosphorus from contaminated water using novel, reusable, renewable resource-based Aluminum/Cerium oxide nanocomposite. *Water Air Soil Poll.*, **231**, 559.
- Pan, G., Lyu, T., Mortimer, R. 2018. Comment: closing phosphorus cycle from natural waters: re-capturing phosphorus through an integrated water-energy-food strategy. *J. Environ. Sci.*, **65**, 375-376.
- Pan, G., Miao, X.J., Bi, L., Zhang, H.G., Wang, L., Wang, L.J., Wang, Z.B., Chen, J., Ali, J., Pan., M.M., Zhang, J., Yue, B., Lyu, T. 2019. Modified local soil (MLS) technology for harmful algal bloom control, sediment remediation, and ecological restoration. *Water*, **11**(6):1123.
- Pan, M., Tao, L., Zhang, M., Zhang, H., Pan, G. 2020. Synergistic Recapturing of External and Internal Phosphorus for In Situ Eutrophication Mitigation. *Water*, **12**(1), 2.
- Ravel, B., Newville, M. 2005. ATHENA, ARTEMIS, HEPHAESTUS: data analysis for

- X-ray absorption spectroscopy using IFEFFIT. *J. Synchrotron Radiat.*, **12**, 537-541.
- Reitzel, K., Lotter, S., Dubke, M., Egemose, S., Jensen, H.S., Andersen, F.Ø. 2013. Effects of Phoslock treatment and chironomids on the exchange of nutrients between sediment and water. *Hydrobiologia*, **703**(1), 189-202.
- Shahat, A., Hassan, M.A., El-Shahat, M.F., Shahawy, O.E., Awual, M. R. 2018. Visual nickel (II) ions treatment in petroleum samples using a mesoporous composite adsorbent. *Chem. Eng. J.*, **334**, 957-967.
- Shin, E.W., Karthikeyan, K.G., Tshabalala, M.A. 2005. Orthophosphate sorption onto lanthanum-treated lignocellulosic sorbents. *Environ. Sci. Technol.*, **39**(16), 6273-6279.
- Shuai Gu, Bitian Fu, Ji-Whan Ahn, Fang, B.Z. 2021. Mechanism for phosphorus removal from wastewater with fly ash of municipal solid waste incineration, Seoul, Korea. *J. Clean. Prod.*, **280**, 124430.
- Smith, V.H., Tilman, G.D., Nekola, J.C. 1999. Eutrophication: impacts of excess nutrient inputs on freshwater, marine, and terrestrial ecosystems. *Environ. Pollut.*, **100**, 179-196.
- Torit, J., Pihusut, D. 2019. Phosphorus removal from wastewater using eggshell ash. *Environ. Sci. Pollut. Res.*, **26**, 34101-34109.
- Van, Oosterhout, F., Lüring, M. 2013. The effect of phosphorus binding clay (Phoslock®) in mitigating cyanobacterial nuisance: a laboratory study on the effects on water quality variables and plankton. *Hydrobiologia*, **710**, 265-277.
- Vassilev, S.V., Vassileva, C.G. 2005. Methods for characterization of composition of fly ashes from coal-fired power stations: a critical overview. *Energy Fuels*, **19**(3), 1084-1098.
- Wan, B., Yan, Y., Fan, L., Tan, W., He, J., Feng, X. 2016. Surface speciation of myo-inositol hexakisphosphate adsorbed on TiO₂ nanoparticles and its impact on their colloidal stability in aqueous suspension: A comparative study with orthophosphate. *Sci. Total Environ.*, **544**(feb.15), 134-142.

- Wang, L.J., Pan, G., Shi, W.Q., Wang, Z.B., Zhang, H.G. 2016a. Manipulating nutrient limitation using modified local soils: a case study at Lake Taihu (China). *Water Res.*, **101**, 25-35.
- Wang, Z., Dong, J., Liu, L., Zhu, G., Liu, C. 2013. Screening of phosphate-removing substrates for use in constructed wetlands treating swine wastewater. *Ecol. Eng.*, **54**, 57-65.
- Wang, Z., Fan, Y., Li, Y.W., Qu, F.R., Wu, D.Y., Nan, K.H. 2016b. Synthesis of zeolite/hydrous lanthanum oxide composite from coal fly ash for efficient phosphate removal from lake water. *Micropor. Mesopor. Mat.*, **222** 226-234.
- White, S.A., Strosnider, W., Chase, M., Schlautman, M.A. 2021. Removal and reuse of phosphorus from plant nursery irrigation return water with reclaimed iron oxides. *Ecol. Eng.*, **160**(1), 106153.
- Xiong, J., Qin, Y., Islam, E., Yue, M., Wang, W. 2011. Phosphate removal from solution using powdered freshwater mussel shells. *Desalination*, **276**, 317-321.
- Xiong, W.H., Peng, J. 2008. Development and characterization of ferrihydrite-modified diatomite as a phosphorus adsorbent. *Water Res.*, **42**, 4869-4877.
- Xu, R., Tao, L., Zhang, M., Cooper, M., Pan, G. 2020. Molecular-level investigations of effective biogenic phosphorus adsorption by a lanthanum/aluminum-hydroxide composite. *Sci. Total Environ.*, **725**, 138424.
- Xu, R., Zhang, M.Y., Mortimer, R., Pan, G. 2017. Enhanced phosphorus locking by novel lanthanum/aluminum-hydroxide composite: implications for eutrophication control. *Environ. Sci. Technol.*, **51**, 3418-3425.
- Yang, J., Yuan, P., Chen, H.Y., Zou, J., Yuan, Z.G., Yu, C.Z. 2012. Rationally designed functional macroporous materials as new adsorbents for efficient phosphorus removal. *J. Mater. Chem.*, **22**(19), 9983-9990.
- Yang, J., Zhou, L., Zhao, L.Z., Zhang, H.W., Yin, J., Wei, G.F., Qian, K., Wang, Y.H., Yu, C.Z. 2011. A designed nanoporous material for phosphate removal with high efficiency. *J. Mater. Chem.*, **21**(8), 2489-2494.
- Yasseri, S., Epe, T.S. 2015. Analysis of the La:P ratio in lake sediments-Vertical and

- spatial distribution assessed by a multiple-core survey. *Water Res.*, **97**, 96-100.
- Zamparas, M., Kyriakopoulos, G.L., Drosos, M., Kapsalis, V.C., Kalavrouziotis, I.K. 2020. Novel composite materials for lake restoration: A new approach impacting on ecology and circular economy. *Sustainability*, **12**(8), 3397.
- Zhang, H.G., Shang, Y.Y., Lyu, T., Chen, J., Pan, G. 2018. Switching harmful algal blooms to submerged macrophytes in shallow waters using geo-engineering methods: evidence from a ¹⁵N tracing study. *Environ. Sci. Technol.*, **52**, 11778-11785.
- Zhang, Y., Pan, B., Chao, S., Xiang, G. 2016. Enhanced phosphate removal by nanosized hydrated La(III) oxide confined in cross-linked polystyrene networks. *Environ. Sci. Technol.*, **50**(3), 1447.

Utilization of coal fly ash waste for effective recapture of phosphorus from waters

Xu, Rui

2021-10-01

Attribution-NonCommercial-NoDerivatives 4.0 International

Xu R, Lyu T, Wang L, et al., (2022) Utilization of coal fly ash waste for effective recapture of phosphorus from waters. *Chemosphere*, Volume 287, Pt 4, January 2022, Article number 132431
<https://doi.org/10.1016/j.chemosphere.2021.132431>

Downloaded from CERES Research Repository, Cranfield University